Talanta 116 (2013) 237–244

Contents lists available at ScienceDirect

Talanta

journal homepage: www.elsevier.com/locate/talanta

Parallel comparative studies on the toxic effects of unmodified CdTe quantum dots, gold nanoparticles, and carbon nanodots on live cells Ćas well as green gram sprouts

Yanchao Song, Duan Feng, Wen Shi, Xiaohua Li, Huimin Ma *

Beijing National Laboratory for Molecular Sciences, Key Laboratory of Analytical Chemistry for Living Biosystems, Institute of Chemistry, ĆChinese Academy of Sciences, Beijing 100190, China

ARTICLE INFO

Article history:
Received 15 March 2013
Received in revised form
9 May 2013
Accepted 11 May 2013
Available online 16 May 2013

Keywords:
CdTe quantum dots
Au nanoparticles
Carbon nanodots
Relative toxicity
Live cells
Fluorescence imaging

ABSTRACT

By using confocal fluorescence microscopy and direct visualization, a parallel comparative investigation has been systematically made on the relative toxicity of three common nanomaterials, such as unmodified CdTe quantum dots (QDs), Au nanoparticles (Au NPs) and carbon nanodots (C-dots), to live cells as well as green gram sprouts. Bare CdTe QDs exert the most toxic effect on a variety of cell lines (HeLa, MCF-7, NIH/3T3 cells) as well as live plants (green gram sprouts). For cells, this toxic effect leads to the partial death of cells, the decrease of cell metabolic activity, the shrinkage of cells, the breakage of chromatin, the damage of cell membrane integrity, and the fragmentation of mitochondria; for green gram sprouts, the presence of CdTe QDs markedly inhibits their growth. Moreover, the toxic behaviors of CdTe QDs are dose- and time-dependent. Under the same conditions, Au NPs only decrease the metabolic activity of cells to a small extent, and do not affect the appearance of cellular/subcellular structures and the plant growth; interestingly, C-dots exert no obvious toxicity to both live cells and the growth of green gram sprouts, showing good biocompatibility. These parallel comparative studies clearly reveal that the relative toxicity of the three nanomaterials in their native forms is bare CdTe QDs≫Au NPs > C-dots, whose IC_{50} values for normal NIH/3T3 cells are 0.98 μg/mL, 62 μg/mL, and > 250 μg/mL, respectively. This quantitative information is of great importance for right choice of the nanomaterials in their practical applications.

1. Introduction

Because of their unique chemical and physical properties, nanomaterials such as CdTe quantum dots (QDs), Au nanoparticles (Au NPs) and carbon nanodots (C-dots), have been widely used in many areas [1–4]. However, one of the major concerns has been raised regarding the toxicity of the nanomaterials in their practical applications like bioimaging and drug delivery. To reveal this, a number of toxicity studies have been conducted both in vitro and in vivo in the past decade [5–8]. Nevertheless, due to the lack of standardized preparation protocols, coatings, doses, and application systems, the observed toxic effects of the nanomaterials are inconsistent. For example, the Cd-containing QDs without coatings show acute damage to cells and tissues in vitro and in vivo [9–13], whereas the Cd-containing QDs that possess a core/shell structure exert little harm on cells [14–16]; the enticing properties of good biocompatibility and low toxicity of Au NPs can be seen in some previous literatures [17,18], but recent evidence has demonstrated that Au NPs can cause cytotoxicity and tissue damage [19,20]; C-dots, as a newly emerging carbon nanomaterial, display good biocompatibility [21,22]. Moreover, most of the existing toxicity studies focused on a single nanomaterial, and did not provide the quantitative information about the relative toxicity of different nanomaterials, such as common CdTe QDs, Au NPs, and C-dots. On the other hand, even though the toxicity of some nanomaterials can be well decreased through multiple inorganic/organic coatings, unavoidable residue in living organisms and eventual degradation to their bare form exist [23,24]. Therefore, parallel comparative investigations of the uncoated (bare) nanomaterials under the same conditions are extremely necessary to better understand their nature and in particular their relative toxicity.

The individual toxicity of CdTe QDs, Au NPs, and C-dots has been extensively studied [10,20,21], but to our knowledge no systematic research has been made on their relative toxicity. Herein, we present such a study by establishing a parallel evaluation method and comparing the toxic effects of these uncoated materials on both live cells and green gram sprouts. Specifically, the effects of CdTe QDs, Au NPs, and C-dots on cell survival and cell

* Corresponding author. Tel.: +86 10 62554673.
E-mail address: mahm@iccas.ac.cn (H. Ma).

0039-9140/$ - see front matter © 2013 Elsevier B.V. All rights reserved.
http://dx.doi.org/10.1016/j.talanta.2013.05.022

metabolic activity were first examined by Hoechst 33342 and 3-(4,5-dimethylthiazol-2-yl)-2,5-diphenyl-tetrazolium bromide (MTT) analyses, and then the progressive changes of the appearance of cellular and sub-cellular structures and plant growth upon treatment with the three nanomaterials were investigated by laser scanning confocal fluorescence imaging and direct visualization. These parallel comparative studies clearly reveal that the relative toxicity of the three nanomaterials in their native forms is bare CdTe quantum dots≫Au nanoparticles > carbon nanodots, whose IC_{50} values for normal NIH/3T3 cells are 0.98 μg/mL, 62 μg/mL, and > 250 μg/mL, respectively. This quantitative information is rather helpful for choosing the suitable nanomaterial in practical applications.

2. Methods

2.1. Materials and apparatus

Tellurium power was purchased from Fluka, and D-(+)-glucose from J & K Chemical Ltd. $HAuCl_4$ was obtained from Beijing Chemicals Ltd, $CdCl_2$ from Alfa Aesar, reduced glutathione (GSH) from Acros, dimethyl sulphoxide (DMSO) and $NaBH_4$ from Sigma-Aldrich. Dulbecco's modified eagle media (DMEM), fetal bovine serum (FBS), penicillin, streptomycin, and phosphate buffered saline (PBS) solution were obtained from Invitrogen Co. MTT was purchased from Serva Electrophoresis GmbH (Germany). Hoechst 33342, propidium iodide, and rhodamine 123 were purchased from Biodee Biotecnology Co., Ltd (Beijing, China). Ultrapure water (over 18 MΩ cm) from a Milli-Q Reference system (Millipore) was used throughout.

Transmission electron microscopy (TEM) images of nanomaterials were taken on a JEM-1011 instrument. UV–vis spectra were recorded in 1-cm quartz cells with a TU-1900 spectrophotometer (Beijing, China). Fluorescence measurements were made on a Hitachi F-2500 fluorescence spectrophotometer (Tokyo, Japan), and dynamic light scattering (DLS) measurements on a Zetasizer nano ZS (ZEN3600) instrument (Malvern, England). MTT analysis and cell number measurement were made on a microplate reader (BIO-TEK Synergy HT, USA).

2.2. Preparation of three nanomaterials

The nanomaterials of unmodified CdTe QDs, Au NPs and C-dots were prepared by the direct aqueous-phase synthesis [25], the trisodium citrate reduction of $HAuCl_4$ [26], and the facile microwave pyrolysis method [27], respectively. Briefly, for CdTe QDs, 8 mg of tellurium powder and 29 mg of sodium borohydride were mixed with 5 mL of nitrogen-saturated water. The mixture was stirred at 0 °C for about 5 h until it became a light-pink color as a sign of the NaHTe formation. At the same time, 0.5 g of $CdCl_2$, 0.42 g of GSH and 125 mL of nitrogen-saturated water were loaded into a 250 mL three-necked flask under stirring, and the pH of solution was adjusted to 11–12 by adding dropwise NaOH solution. The flask was sealed, and the NaHTe solution prepared above was injected into the mixture via a syringe under nitrogen atmosphere. The reaction mixture was slowly heated to 100 °C under N_2 and stirred for 3 h. The CdTe QDs were separated as a precipitate by adding ethanol to the reaction mixture. Then, the precipitate was washed several times with ethanol, and ethanol was removed by rotary evaporation.

For Au NPs, 50 mL of aqueous $HAuCl_4$ (0.25 mM) solution was heated to reflux with vigorously stirring and 1.3 mL of trisodium citrate (1%, w/v) was then added into the solution rapidly. The color of solution changed from light yellow to wine red in about 3 min, indicating the formation of Au NPs. The solution was cooled to room temperature with continuous stirring and then stored in a refrigerator at 4 °C for future use. The concentrated Au NPs solution can be obtained by centrifugation, and the concentration of Au NPs in solution can be determined by weighing their solid form that was obtained via lyophilization of a parallel solution.

For C-dots, glucose (2 g) was dissolved in water (3 mL), and the mixture was sonicated for 5 min to form a clear solution. Then the solution was heated for 10 min in a 500 W microwave oven with a frequency of 2450 MHz, yielding a dark brown solution. The reaction solution was purified via continuous dialysis (a membrane with molecular weight cutoff of approximately 1000) for 24 h, affording a brown solution (i.e., the bare C-dots), which was kept at 4 °C for future use. The concentration of C-dots in solution can be determined by weighing their solid form that was obtained via lyophilization of a parallel solution.

2.3. Measurement of cell survival

A calibration curve of Hoechst 33342 fluorescence intensity as a function of cell number was made in order to determine the cell survival after a nanomaterial treatment. Briefly, cells were seeded in 96-well U-bottom plates at a density of 7000 cells/well, and incubated with one of the three nanomaterials at varied concentrations at 37 °C for 24 h. Then, the culture media were discarded, a culture medium containing Hoechst 33342 (final concentration was 10 μM) was added, and the cells were incubated at 37 °C for 30 min. After this, the cells were washed with PBS to remove the free Hoechst 33342, followed by lysis with DMSO. The fluorescence of the sample and the control group untreated with the nanomaterial was measured at λex/em = 350/461 nm by using microplate reader. All the measurements were done in five independent experiments. The relative cell number (*CN*) was calculated according to the equation of $CN = F/F_0 \times 100\%$, where F and F_0 are the fluorescence of the experimental group (i.e., the cells were treated with the nanomaterial) and the control group (i.e., the cells were untreated with the nanomaterial), respectively.

2.4. MTT assay

The cytotoxicity of nanomaterials to cells was evaluated by the standard MTT assay. Briefly, cells were seeded in 96-well U-bottom plates at a density of 7000 cells/well, and incubated with one of the three nanomaterials at varied concentrations at 37 °C for 24 h. Then, the culture media were discarded, and 0.1 mL of DMEM solution containing 0.5 mg/mL of MTT was added to each well, followed by incubation at 37 °C for 4 h. The supernatant was abandoned, and 110 μL of DMSO was added to each well to dissolve the formed formazan. After shaking the plates for 5 min, absorbance values of the wells were read with a microplate reader at 490 nm. The cell viability rate (*VR*) was calculated according to the equation: $VR = A/A_0 \times 100\%$, where A and A_0 are the absorbance of the experimental group (i.e., the cells were treated with the nanomaterial) and the control group (i.e., the cells were untreated with the nanomaterial), respectively.

2.5. Cell imaging

Unless otherwise stated, HeLa, MCF-7 and NIH-3T3 cells used in this study were cultured in DMEM containing 10% (v/v) fetal bovine serum and 1% (v/v) penicillin–streptomycin at 37 °C in a 5% CO_2 incubator. The adherent cells were grown on glass-bottom culture dishes (MatTek Co.) containing 1 mL of culture media. Before use, the cells were washed three times with serum-free DMEM. The nanomaterial of CdTe QDs, Au NPs, or C-dots with varied concentrations was added in parallel to different dishes containing the washed cells in DMEM, and the cells were incubated for 24 h. After the culture media were discarded, the cells were washed three times with PBS solution (pH 7.4), followed by

incubation in DMEM with different dyes (10 μM Hoechst 33342 at 37 °C for 40 min, 7.5 μM propidium iodide at 4 °C for 10 min, and 1 μM rhodamine 123 at 37 °C for 2 min). Then the cells were washed with PBS solution (pH 7.4) for imaging experiments. Specifically, cell nuclei were stained with the dye Hoechst 33342, and the fluorescence imaging was made with excitation at 405 nm and a variable bandpass emission filter setting to 425–525 nm; plasma membrane damage was investigated by incubating with propidium iodide and imaging the cells with excitation at 559 nm and the bandpass emission filter setting to 575–675 nm; mitochondria were stained with rhodamine 123, and the fluorescence imaging was made with excitation at 515 nm and the bandpass emission filter setting to 535–635 nm.

In another set of experiments, cells were treated in parallel with the nanomaterials at a fixed concentration (25 μg/mL) for different time. Then the cells were incubated with different dyes and imaged as above. Imaging experiments were made on a FV 1000-IX81 confocal laser scanning microscope (Olympus, Japan) with FV5-LAMAR through a 100 × 1.4 NA objective. Optical sections were acquired at 0.8 μm. The change of cell morphology was analyzed by differential interference contrast (DIC) images.

2.6. Effects of different nanomaterials on the growth of green gram sprouts

Green grams (Phaseolus radiaus L.), obtained from the supermarket, were sowed in different 60 mm × 15 mm dishes (CORNING Co.), and covered with pure water (control) and aqueous solution of 25 μg/mL CdTe QDs, Au NPs, or C-dots, respectively. Then, the dishes were placed for different periods of time at room temperature (about 25 °C) without lids so as to make sure the sufficient oxygen supply. During the seed germination process, if necessary, appropriate water was supplemented to the dishes to keep the fixed volume of solution due to the evaporation. The averaged length ($n=5$) of bean sprouts was measured, and their growth situation was photographed.

3. Results and discussion

3.1. Characterization of three nanomaterials

Common CdTe QDs, Au NPs, and C-dots were chosen as representative nanomaterials in our study because of their wide applications. As mentioned above, all these materials can be obtained by ready preparation methods, such as direct aqueous-phase QDs synthesis, trisodium citrate reduction of $HAuCl_4$, and microwave pyrolysis. Moreover, their unmodified or bare forms were used to reflect the real toxicity, considering the fact that modified nanomaterials are unavoidably degraded to their bare forms to reside and accumulate in the corresponding application fields such as living organisms or environments [23,24]. Physicochemical properties of the as-prepared nanomaterials were characterized with various techniques. Firstly, their size and morphology were investigated by TEM analysis. As shown in Fig. 1A, the nanomaterials are uniform and nearly round. The size distributions of CdTe QDs, Au NPs, and C-dots are in the range of 1–5, 12–19, and 1–4 nm (Fig. 1B), respectively. Secondly, average hydrodynamic diameter and zeta-potential of the nanomaterials were examined by dynamic light scattering analysis. As depicted in Table 1, the average hydrodynamic diameters of CdTe QDs, Au NPs and C-dots are 3.9, 22, and 3.0 nm (Fig. S1), respectively, which are actually close to the TEM characterizations because hydrodynamic diameter is usually slightly larger than the dry-state diameter. The zeta-potential values of CdTe QDs, Au NPs and C-dots are −24, −10, and −5.2 mV (Table 1), respectively. The negatively charged features may result from the presence of reduced glutathione [25], citrate ions, and the formed carboxyl/hydroxyl groups during the microwave pyrolysis process, on the surface of CdTe QDs, Au NPs, and C-dots, respectively. Moreover, these nanomaterials were also characterized by UV-visible spectra and fluorescence spectra (Fig. S2), the Au NPs display an absorption maximum at 520 nm, the CdTe QDs from heat treatment of 3 h exhibit a single narrow emission peak at 570 nm, and the C-dots demonstrate a typical emission shift with the change of excitation wavelength, all of which suggest the successful preparation of the nanomaterials.

Table 1
Hydrodynamic diameter and zeta-potential of CdTe QDs, Au NPs, and C-dots from dynamic light scattering analysis.

Nanomaterial	Hydrodynamic diameter (nm)	Zeta-potential (mV)
CdTe QDs	3.9	–24
Au NPs	22	–10
C-dots	3.0	–5.2

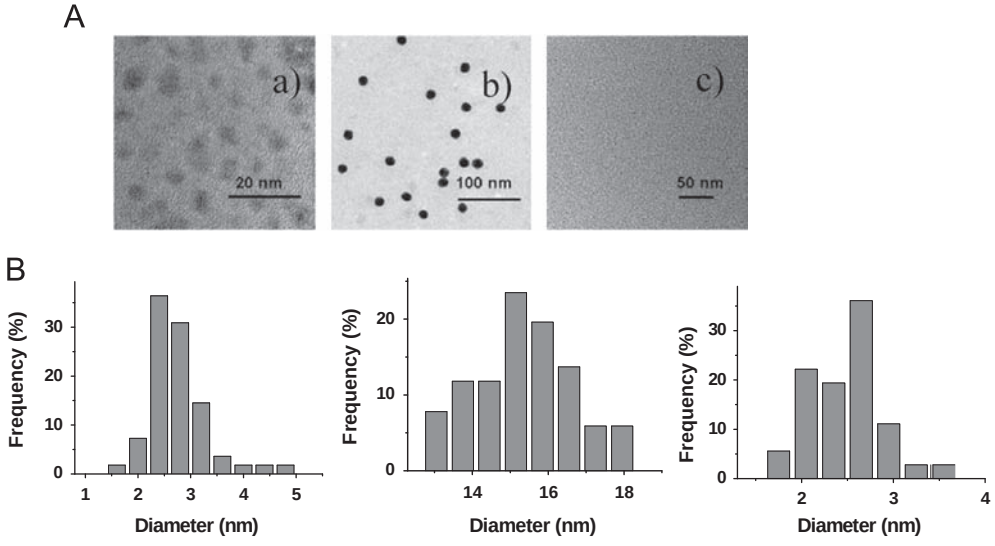

Fig. 1. (A) TEM images of (a) CdTe QDs, (b) Au NPs, and (c) C-dots. (B) Diameter distribution of the particles from the above corresponding TEM images.

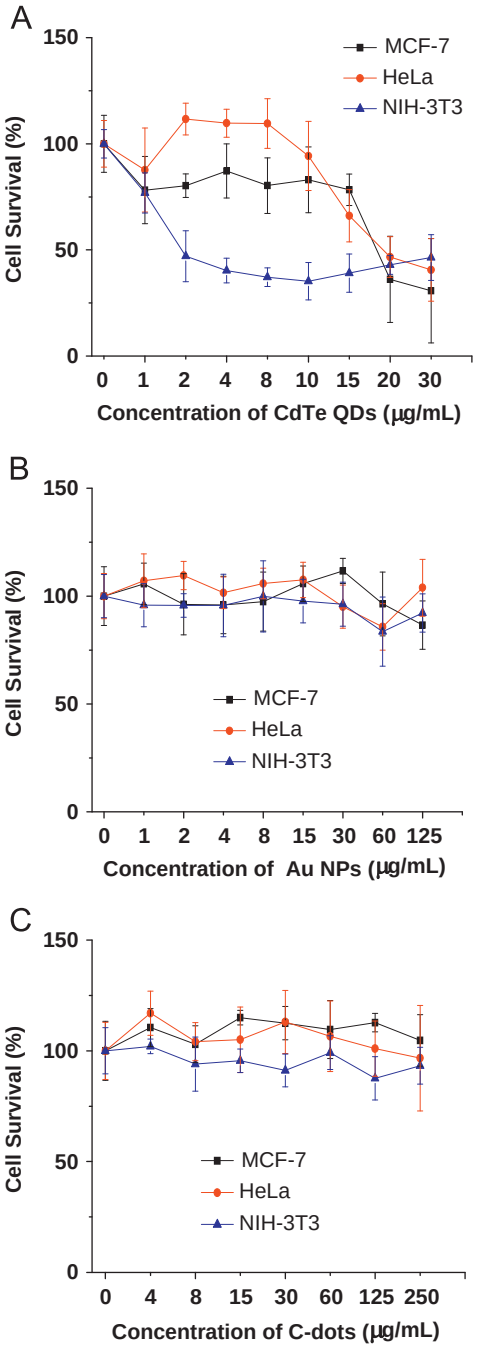

Fig. 2. The cell survival changes after 24 h of incubation with (A) CdTe QDs, (B) Au NPs, and (C) C-dots at different concentrations (the cell survival without treatment by the nanomaterials is defined as 100%). The results were the mean ± SD of 5 separate measurements.

3.2. *Effects of the nanomaterials on cell survival*

The toxic effect of different nanomaterials on the change of cell number was investigated by using Hoechst 33342 fluorescence and correlating it with a calibration curve of a known number of cells (Fig. 2), because cell survival as the most common indicator can reflect an integrated toxicological effect. As shown in Fig. 2A, CdTe QDs cause a remarkable decline in the cell number for all types of cells (MCF-7, HeLa and NIH/3T3 cells) in a dose-dependent manner, i.e., when the concentrations of CdTe QDs increase from 0 to 30 μg/mL in the culture media a gradual decrease in the cell number is observed. It is noteworthy that the number of NIH/3T3 cells decreases almost by 50% when they were exposed to 2 μg/mL of CdTe QDs, though the cell survival no longer changes greatly at higher concentrations of CdTe QDs; however, for the cancer cells (i.e. MCF-7 and HeLa cells), 50% cell survival is found at a concentration as high as about 20 μg/mL of CdTe QDs. The reason for this may be ascribed to the fact that cancer cells usually have stronger surviving ability in various environments. Interestingly, both Au NPs (Fig. 2B) and C-dots (Fig. 2C) scarcely affect the cell numbers. For instance, the average cell loss from the tested three

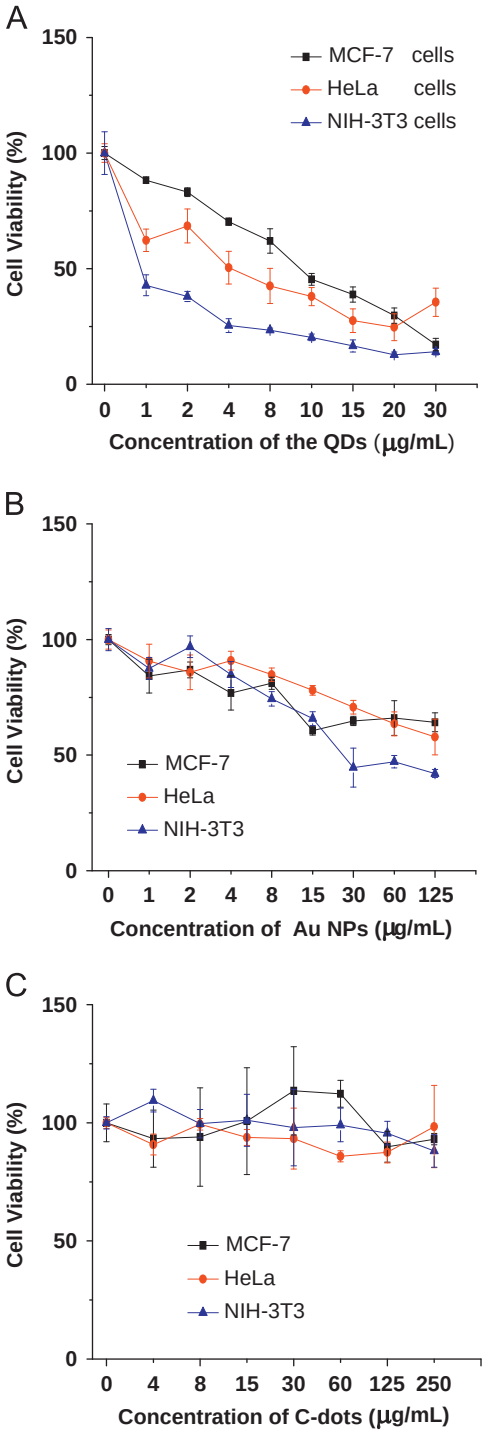

Fig. 3. The cell viability changes after 24 h of incubation with (A) CdTe QDs, (B) Au NPs, and (C) C-dots at varied concentrations (the viability of the cells in the absence of the nanomaterial is defined as 100%). The results were the mean ± SD of 5 separate measurements.

types of cells is less than 10% even when they were exposed to 125 μg/mL of Au NPs or 250 μg/mL of C-dots.

3.3. Studies on the metabolic activity by MTT assay

The standard MTT assay was made to measure the cell metabolic activity following the previous approach [2,27]. As shown in Fig. 3, CdTe QDs exert the most toxic effect on all types of cells, among which NIH/3T3 cells are affected most seriously. Moreover, this toxic effect behaves in a dose-dependent manner (Fig. 3A), i.e., with the increase of the CdTe QDs concentration the metabolic activity decreases accordingly, similar to the above cell survival result. Although the exact toxic mechanism remains to be resolved, a possible explanation may be due to the release of Cd^{2+} ions present at particle surface, which probably changes the oxidative stress in biosystems [10,28].

For Au NPs, increase of their concentration also leads to the gradual decrease in the metabolic activity of the cells (Fig. 3B), but this decrease is not as intense as that by CdTe QDs. For example, the increase of Au NPs concentration to 1 μg/mL only gives rise to about 10% decrease in the averaged metabolic activity of the three types of cells. Nevertheless, this concentration of 1 μg/mL Au NPs almost causes no cell loss (see the above Fig. 2B), suggesting that Au NPs do not alter the cell number but indeed affect the metabolic activity significantly. The reason for this toxic effect may be attributed to the interactions of Au NPs with proteins and vital cell components such as the membrane, mitochondria, or nucleus, which causes the change of not only the effective surface charge of proteins but also the apoptotic rate of cells [29,30].

Compared to CdTe QDs and Au NPs, C-dots even at a concentration as high as 250 μg/mL hardly exhibit an effect on the cell metabolic activity (Fig. 3C). This good biocompatibility may be ascribed to that C-dots mainly contain carbon, hydrogen and oxygen that are not toxic elements, as described previously [21]. To quantitatively compare the relative toxicity of the nanomaterials, the IC_{50} values of CdTe QDs, Au NPs, and C-dots for normal NIH/3T3 cells were determined to be 0.98 μg/mL, 62 μg/mL, and >250 μg/mL, respectively, based on the MTT analytical data. The above results clearly show that the toxicity of the nanomaterials is CdTe QDs≫Au NPs > C-dots.

3.4. Laser scanning confocal fluorescence imaging

In this study HeLa cells were chosen as model cells, because they are the most commonly used ones in fluorescence imaging experiments. Specifically, upon treatment of HeLa cells with the three nanomaterials, the progressive changes of the appearance of cellular and sub-cellular structures, including cell morphology, cell nuclei and chromatin shapes, cell membrane integrity, and mitochondria appearance, were systematically investigated by laser scanning confocal fluorescence imaging.

3.4.1. Effects of nanomaterials on cell morphology

Upon treatment with the nanomaterials, the change of cell morphology was first analyzed by DIC images (Fig. 4). The untreated HeLa cells (control) have a polygonal morphology, and the cell nucleolus structures can be easily distinguished as the bulgy dots, one of which is pointed out by the white arrow in the enlarged yellow box in the control of row A. For CdTe QDs, a clear dose-dependent effect on cell morphology is observed (row A in Fig. 4): 5 μg/mL of CdTe QDs does not cause an obvious change, but 10 μg/mL of CdTe QDs leads to the cell shrinkage and the indistinguishable nucleolus structure; 25 μg/mL of CdTe QDs could induce the cytoplasmic blebbing, which indicates cell apoptosis. Higher concentrations of CdTe QDs, such as 50 μg/mL, even can destroy the adherent cells, resulting in their disappearance in the visual field (the last image of row A in Fig. 4).

Treatment of the cells with Au NPs does not change the cell morphology noticeably, but irregular black color can be visualized on the cells when higher concentrations (>10 μg/mL) of Au NPs were used. This phenomenon might arise from the adsorbed Au NPs, similar to the known observations [29,31,32]. Under the same conditions, C-dots up to 50 μg/mL did not influence the cell morphology, consistent with the above finding that C-dots have the lowest toxicity.

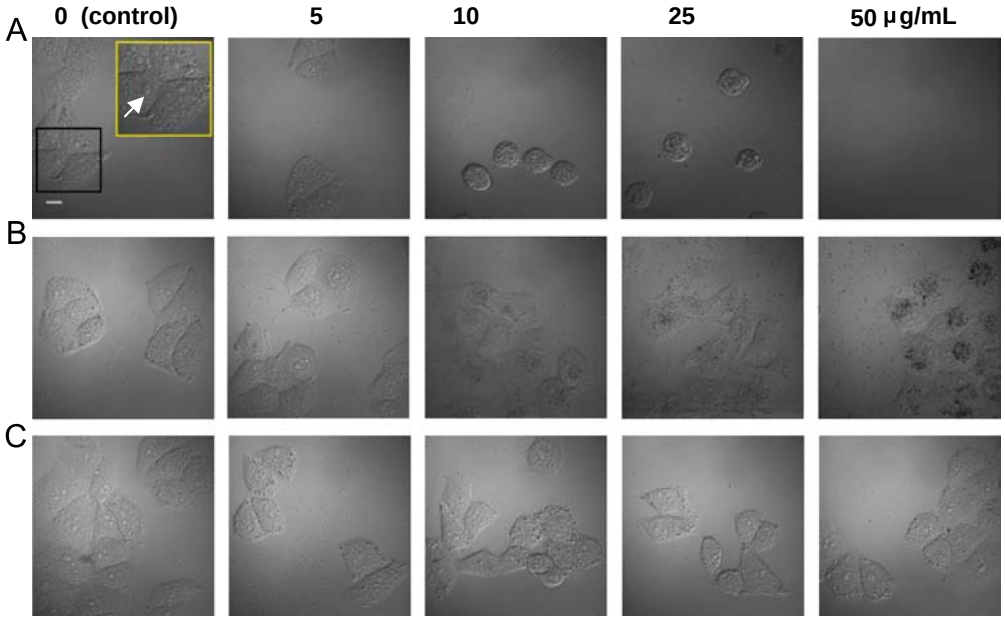

Fig. 4. DIC images of HeLa cells treated at 37 °C for 24 h with different nanomaterials (A: CdTe QDs; B: Au NPs; C: C-dots) at various concentrations (0, 5, 10, 25, and 50 μg/mL). In the first image of row A, the yellow box depicts the magnified version of the black box, in which the white arrow indicates one of the cell nucleolus structures. Scale bar, 10 μm. (For interpretation of the references to color in this figure legend, the reader is referred to the web version of this article.)

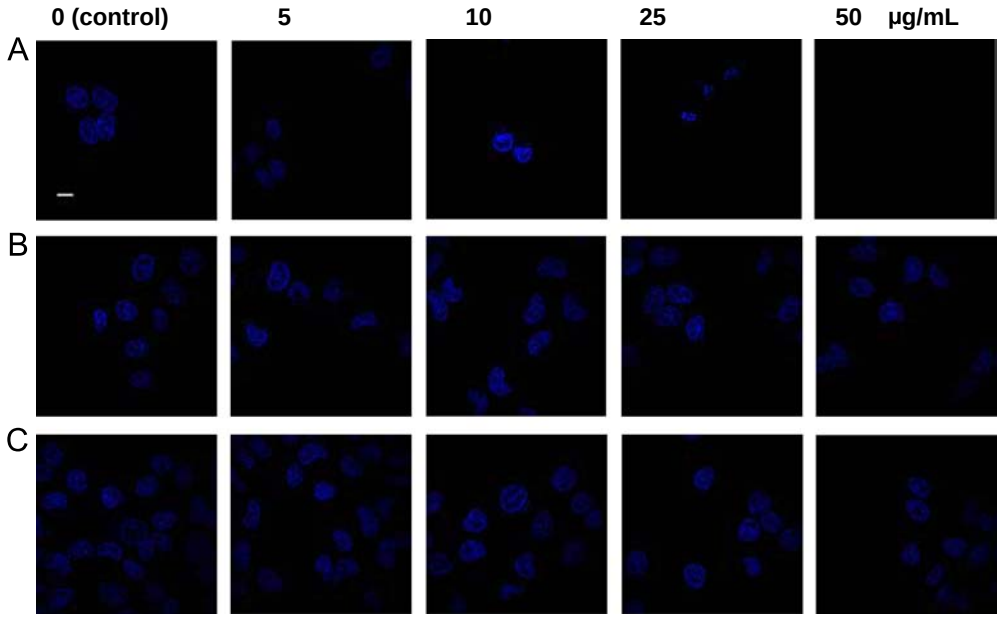

Fig. 5. Fluorescence images of the cell nuclei of HeLa cells. The cells were first treated at 37 °C for 24 h with different nanomaterials (A: CdTe QDs; B: Au NPs; C: C-dots) at various concentrations (0, 5, 10, 25, and 50 μg/mL), and then incubated with Hoechst 33342 at 37 °C for 40 min. Scale bar, 10 μm.

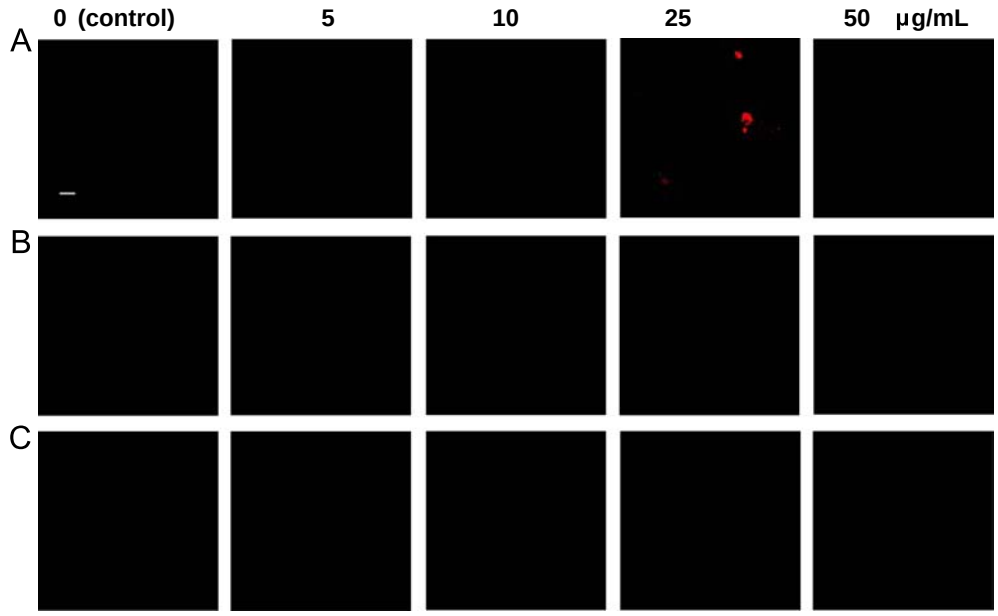

Fig. 6. Fluorescence images of the membrane integrity of HeLa cells. The cells were first treated at 37 °C for 24 h with different nanomaterials (A: CdTe QDs; B: Au NPs; C: C-dots) at various concentrations (0, 5, 10, 25, and 50 μg/mL), and then incubated with propidium iodide at 4 °C for 10 min. Scale bar, 10 μm.

3.4.2. Effects of nanomaterials on cell nuclei

The effects of nanomaterials on cell nuclei were studied by imaging the stained cell nuclei with the specific dye Hoechst 33342. As shown in Fig. 5, control group exhibit oval or dumbbell shapes with irregular blue fluorescence, which is attributed to the presence of both heterochromatin and euchromatin. It is noted that the nuclei membrane is clearly visible. However, the cells treated with 5 μg/mL of CdTe QDs show a slight shrinkage of the nuclei, and 10 μg/mL of CdTe QDs leads to a partial aggregation of chromatin with much brighter fluorescence. This increased fluorescence possibly results from the severe damage of cells and thus more dye entrance. Higher concentrations of CdTe QDs, such as ≥25 μg/mL, could cause the fragmentation of chromatin and even cell death (i.e., no adherent cells), respectively, revealing that CdTe QDs also show a dose-dependent damage on cell nuclei.

In contrast, both Au NPs and C-dots up to 50 μg/mL did not show any obvious influence on the cell nuclei compared to the control group (Fig. 5).

3.4.3. Effects of nanomaterials on cell membrane

Cell membrane integrity is a sign of cell health. In our study, the damage degree of cell membrane upon treatment with the nanomaterials was investigated by using the dye propidium iodide, which can enter the cells to specifically stain the cell nuclei only after the cell membrane is damaged [12]. As shown in Fig. 6, CdTe QDs at a concentration of lower than 10 μg/mL do not affect the cell membrane integrity considerably, because no obvious fluorescence is observed. Nevertheless, the nuclei of HeLa cells treated with 25 μg/mL of CdTe QDs produce bright red

fluorescence, indicating the damage of the intact cell membrane and thus the entrance of propidium iodide. Similarly, higher dosages of CdTe QDs, like 50 μg/mL, can result in the death of the cells. Interestingly, both Au NPs and C-dots up to 50 μg/mL show little effect on the cell membrane integrity.

3.4.4. *Effects of nanomaterials on mitochondria*

The effects of nanomaterials on mitochondria were examined by imaging the stained mitochondria with the specific dye rhodamine-123. As depicted in Fig. 7, in the absence of nanomaterials the interconnected tubular shape mitochondria show bright fluorescence and distribute in the cell cytoplasm. After exposed to CdTe QDs at an increasing concentration from 5 to 25 μg/mL, the fluorescing spots are gradually decreased (Fig. 7), suggesting the fragmentation of the mitochondria, which is the early sign of cell apoptosis [33–35]. The dosage of 50 μg/mL CdTe QDs causes the death of all the cells. Au NPs up to 50 μg/mL did not show a significant influence on the mitochondria appearance of HeLa cells (Fig. 7), but indeed decreased the succinodehydrogenase activity in mitochondria by about 40%, as demonstrated in the above MTT assay. Differently, C-dots did not cause the changes in both succinodehydrogenase activity and mitochondria appearance in the cells (Fig. 7).

On the other hand, the effects of incubation time of the nanomaterials at a constant concentration of 25 μg/mL were investigated on HeLa cells. As shown in Figs. S3–S6, with the increase of incubation time from 0 to 24 h, CdTe QDs display a gradually increased influence on the cells, including cell morphology and nuclear shrinkage, cell membrane damage and mitochondria fragmentation. Under the same conditions, however, both Au NPs and C-dots did not significantly affect the cell morphology, cell nuclear shape, cell membrane integrity, and mitochondria appearance. This further supports the above observation that CdTe QDs have the highest toxicity to the cells, and this toxicity is time-dependent.

3.5. *Effects of the nanomaterials on the growth of green gram sprouts*

To further understand the relative toxicity, the effects of CdTe QDs, Au NPs, and C-dots were also examined on the growth of live plants such as green gram sprouts, which are sensitive to toxins and can reflect the toxicity at the early stage of exposure. In this experiment, green grams were simultaneously sowed in different culture media, which were pure water (control) and the aqueous solutions of CdTe QDs, Au NPs and C-dots with the same concentration of 25 μg/mL, respectively. Then, the growth situations of green gram sprouts with time were photographed, and the averaged growth lengths of the green gram sprouts were measured. Fig. S7 shows some typical growth situations of the green gram sprouts with time. As can be seen, the little sprouts are gown out of green grams in all groups after 24 h, but no obvious difference is observed during the first 48 h growth. However, differences occur after 60 h growth: green gram sprouts in the CdTe QDs solution grow much slower than those in the other three groups. Interestingly, the growth situation of green gram sprouts in either Au NPs or C-dots solution is still indistinguishable from that in water (control group). Fig. 8 shows the detailed comparison of the averaged growth lengths ($n=5$) of green gram sprouts in all the four groups, which clearly reveals that CdTe QDs exert the most remarkable inhibition on the growth of green gram sprouts, whereas Au NPs and C-dots show little effect.

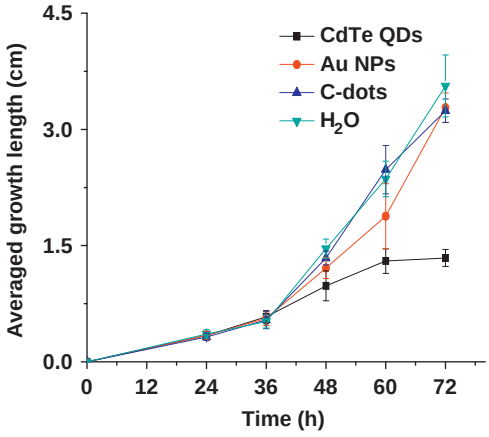

Fig. 8. The averaged growth length ($n=5$) of green gram sprouts with time in different culture media.

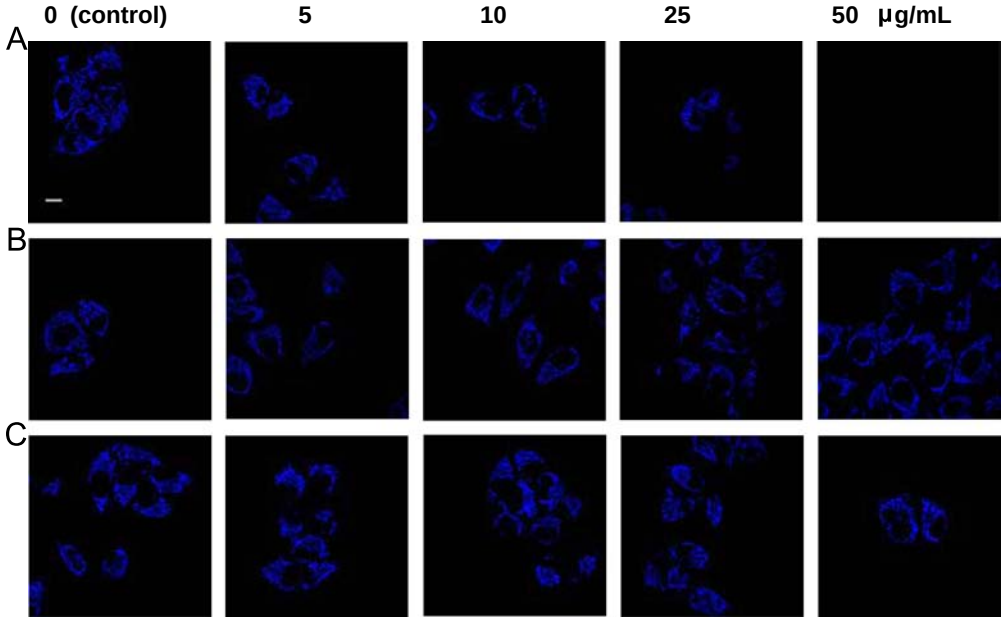

Fig. 7. Fluorescence images of mitochondria of HeLa cells. The cells were first treated at 37 °C for 24 h with different nanomaterials (A: CdTe QDs; B: Au NPs; C: C-dots) at various concentrations (0, 5, 10, 25, and 50 μg/mL), and then incubated with rhodamine-123 at 37 °C for 2 min. Scale bar, 10 μm.

4. Conclusion

In view of the increasing biomedical and environmental safety concerns, the relative toxicity of three common bare nanomaterials (CdTe QDs, Au NPs and C-dots) to live cells and green gram sprouts has been systematically investigated under the same conditions. The results demonstrated that CdTe QDs show the highest toxicity to live cells and plant growth. Au NPs only at higher concentrations (>1 μg/mL) inhibit significantly the cell metabolic activity. Compared to CdTe QDs and Au NPs, however, C-dots scarcely exert any serious effect on both live cells and plant growth. These parallel comparative studies clearly indicate that the relative toxicity of the nanomaterials is bare CdTe QDs≫Au NPs > C-dots, and their IC_{50} values for normal NIH/3T3 cells are 0.98 μg/mL, 62 μg/mL, and >250 μg/mL, respectively. The present toxicity observations (in particular the high toxicity of CdTe QDs) should arouse sufficient attention, and we believe that these results are of great importance for right choice of the nanomaterials in their practical applications.

Acknowledgments

We are grateful to the financial support from the NSF of China (Nos. 20935005, 21275146, 21275147 and 21105104), the 973 Program (2011CB935800), and the Chinese Academy of Sciences (KJCX2-EW-N06-01).

Appendix A. Supporting information

Supplementary data associated with this article can be found in the online version at http://dx.doi.org/10.1016/j.talanta.2013.05.022.

References

[1] M. Xue, X. Wang, H. Wang, Bo Tang, Talanta 83 (2011) 1680–1686.
[2] W. Shi, X.H. Li, H.M. Ma, Angew. Chem. Int. Ed. 51 (2012) 6432–6435.
[3] M. Kim, J.H. Seo, W. Jeon, M.Y. Kim, K.C. Cho, S.Y. Lee, S.W. Joo, Talanta 88 (2012) 631–637.
[4] J. Ai, Y.H Xu, D. Li, Z.J. Liu, E.K. Wang, Talanta 101 (2012) 32–37.
[5] S. Sharifi, S. Behzadi, S. Laurent, M.L. Forrest, P. Stroeve, M. Mahmoudi, Chem. Soc. Rev. 41 (2012) 2323–2343.
[6] A. Nagy, A. Steinbruck, J. Gao, N. Doggett, J.A. Hollingsworth, R. Lyer, ACS Nano 6 (2012) 4748–4762.
[7] L.B. Du, X.X. Miao, H.Y. Jia, Y.L. Gao, K. Liu, X.J. Zhang, Y. Liu, Talanta 101 (2012) 11–16.
[8] J. Zhu, L. Liao, L. Zhu, P. Zhang, K. Guo, J.L. Kong, C. Ji, B.H. Liu, Talanta 107 (2013) 408–415.
[9] B.R. Singh, B.N. Singh, W. Khan, H.B. Singh, A.H. Naqvi, Biomaterials 33 (2012) 5753–5767.
[10] A. Ambrosone, L. Mattera, V. Marchesano, A. Quarta, A.S. Susha, A. Tino, A.L. Rogach, C. Tortiglione, Biomaterials 33 (2012) 1991–2000.
[11] Y. Qu, W. Li, Y.L. Zhou, X.F. Liu, L.L. Zhang, L.M. Wang, Y.F. Li, A. Iida, Z.Y. Tang, Y.L. Zhao, Z.F. Chai, C.Y. Chen, Nano Lett. 11 (2011) 3174–3383.
[12] L. Jasmina, J.C. Sung, M.W. Francoise, M. Dusica, Chem. Biol. 12 (2005) 1227–1234.
[13] K.G. Li, J.T. Chen, S.S. Bai, X. Wen, S.Y. Song, Q. Yu, J. Li, Y.Q. Wang, Toxicol. In Vitro 23 (2009) 1007–1013.
[14] M. Vibin, R. Vinayakan, A. John, V. Raji, C.S. Rejiya, N.S. Vinesh, A. Abraham, J. Nanopart. Res. 13 (2011) 2587–2596.
[15] Y.Y. Su, Y. He, H.T. Lu, L.M. Sai, Q.N. Li, W.X. Li, L.H. Wang, P.P. Shen, Q. Huang, C.H. Fan, Biomaterials 30 (2009) 19–25.
[16] J.X. Lu, Y.C. Song, W. Shi, X.H. Li, H.M. Ma, Chin. J. Chem. 31 (2013) 472–478.
[17] M.C. Daniel, D. Astruc, Chem. Rev. 104 (2004) 293–346.
[18] Q. Zhang, V.M. Hitchins, A.M. Schrand, S.M. Hussain, Nanotoxicology 5 (2011) 284–295.
[19] M.A. Abdelhalim, Lipids Health Dis. 10 (2011) 205.
[20] S.J. Soenen, B. Manshian, J.M. Montenegro, F. Amin, B. Meermann, T. Thiron, M. Cornelissen, F. Vanhaecke, S. Doak, W.J. Parak, S.D. Smedt, K. Braeckmans, ACS Nano 6 (2012) 5767–5783.
[21] S.T. Yang, X. Wang, H.F. Wang, F.S. Lu, P.G. Luo, L. Cao, M.J. Meziani, J.H. Liu, Y.F. Liu, M. Chen, Y.P. Huang, Y.P. Sun, J. Phys. Chem. C 113 (2009) 18110–18114.
[22] S.N. Qu, X.Y. Wang, Q.P. Lu, X.Y. Liu, L.J. Wang, Angew. Chem. Int. Ed. 51 (2012) 12215–12218.
[23] D. Maysinger, J. Lovric, A. Eisenberg, R. Savic, Eur. J. Pharm. Biopharm. 65 (2007) 270–281.
[24] A.M. Derfus, W.C. Chan, S.N. Bhatia, Nano Lett. 4 (2004) 11–18.
[25] W.C. Law, K.T. Yong, I. Roy, H. Ding, R. Hu, W.W. Zhao, P.N. Prasd, Small 5 (2009) 1302–1310.
[26] D. Feng, Y.Y. Zhang, W. Shi, X.H. Li, H.M. Ma, Chem. Commun. 46 (2010) 9203–9205.
[27] Y.C. Song, W. Shi, W. Chen, X.H. Li, H.M. Ma, J. Mater. Chem. 22 (2012) 12568–12573.
[28] A. Cuypers, M. Plusquin, T. Remans, M. Jozefczak, E. Keunen, H. Gielen, K. Opdenakker, A.R. Nair, E. Munters, T.J. Artois, T. Nawrot, J. Vangronsveld, K. Smeets, Biometals 23 (2010) 927–940.
[29] S.Y. Choi, S. Jeong, S.H. Jang, J. Park, J.H. Park, K.S. Ock, S.Y. Lee, S.W. Joo, Toxicol. In Vitro 26 (2012) 229–237.
[30] A.M. Alkilany, C.J. Murphy, J. Nanopart. Res. 12 (2010) 2313–2333.
[31] C. Freese, C. Uboldi, M.I. Gibson, R.E. Unger, B.B. Weksler, I.A. Romero, P.O. Couraud, C.J. Kirkpatrick, Part. Fibre Toxicol 9 (2012) 23.
[32] C. Freese, M.I. Gibson, H.A. Klok, R.E. Unger, C.J. Kirkpatrick, Biomacromolecules 13 (2012) 1533–1543.
[33] D.L. Wang, J.N. Wang, G.M. Bonamy, S. Meeusen, R.G. Brusch, C. Turk, P.Y. Yu, P.G. Schultz, Angew. Chem. Int. Ed. 51 (2012) 9302–9305.
[34] J. Estaquier, D. Arnoult, Cell Death Differ. 14 (2007) 1086–1094.
[35] T. Landes, J.C. Martinou, Biochim. Biophys. Acta 2011 (1813) 540–545.